ELECTRICAL IMPEDANCE TOMOGRAPHY AND A RESISTIVE NETWORK

by

YONG JUNG KIM AND MIN-GI LEE

Applied Mathematics
Research Report
08 - 05
December 23, 2008

DEPARTMENT OF MATHEMATICAL SCIENCES

KAIST 한국과학기술원
Korea Advanced Institute of Science and Technology

ELECTRICAL IMPEDANCE TOMOGRAPHY AND A RESISTIVE NETWORK

YONG JUNG KIM* AND MIN-GI LEE†

Abstract. In this paper we introduce a non-iterative method to recover a static conductivity image from internal currents and the boundary conductivity. The domain of the conductivity body is approximated as a resistive network and a direct method to recover the conductivity image is suggested which is based on the Kirchhoff laws of voltage and current. The conductivity tensors are diagonal matrices in a semi-anisotropic case and the method shows that rectangular resistive networks perfectly fit to the case. This algorithm has a low computational cost and three dimensional computations can be easily performed. The stability of the method is given in terms of the condition number of a matrix given by the currents that flow the network. A large part of the paper is about numerical stability test of the method. Numerical examples in two and three space dimensions are given for various tests.

Key words. electrical impedance tomography, electrical density image, magnetic resonance image, reconstruction, resistive network, anisotropic conductivity, Kirchhoff's laws, inverse problem

AMS subject classifications. 34K29, 35R30

1. Introduction.

The conductivity of a body decides the interior electrical current when a boundary injection current is given. Finding conductivity images has a tremendous importance, in particular, if a human body is the target. For example, the biological tissues have various micro- and macroscopic structures and the electrical properties are affected by them. Hence the conductivity image of a body may provide valuable diagnostic information. Another example is the defibrillation that applies an electric current to the heart to restore normal rhythm after fibrillation has occurred. If the conductivity is known even for an exemplary case, it will help to develop an efficient way to maximize the effect and to minimize the damage to other organs after the therapy.

In the electrical impedance tomogrphy (EIT) one injects various kinds currents to a body and measures the boundary voltages to construct images of the conductivity. The EIT technique has been actively studied since early 1980s (see [19, 22] and references therein). Classical image reconstruction algorithms are to iteratively update the conductivity image to minimize the observed and computed boundary voltages [6, 23, 24] or to produce images of changes of conductivity generated by cardiac or respiratory functions [8, 9]. This inverse problem is a well-known ill-posed problem [1, 7, 18] due to the insensitivity of the change of the boundary voltage to the change of interior conductivity and the spacial resolution of reconstructed conductivity images are poor. However, the technique is successfully applied to the anomaly detection [3, 4, 5]. Efforts to improve the resolution of EIT can be found in [2] and references therein.

On the other hand techniques that measure the internal current distribution have been developed to obtain high resolution static conductivity images. These techniques employ magnetic resonance imaging (MRI) scanners to obtain internal current. These

*KAIST, Department of Mathematical Sciences, 335 Gwahangno, Yuseong-gu, Daejeon, 305-701, Republic of Korea. (yongkim@kaist.edu). This author was supported by the Korea Science and Engineering Foundation(KOSEF) grant funded by the Korean government(MOST) (No. R01-2007-000-11307-0).

†KAIST, Department of Mathematical Sciences, 335 Gwahangno, Yuseong-gu, Daejeon, 305-701, Republic of Korea. (imingi@kaist.ac.kr).

are used to obtain current density images in MRCDI [10, 11, 12, 20, 21] or conductivity images in MREIT [13, 14, 15, 16, 17]. Recently a technique based on the analysis of equipotential lines has been proposed [19] to reconstruct a conductivity image using a single set of internal current and boundary voltage.

We have two main goals in developing conductivity reconstruction method. The first one is to obtain a stable method. The insensitivity of the inverse problem is reduced if the internal current is measured. However, the problem is still insensitive on the change of the conductivity. Hence it is important to avoid possible sources of instability in the reconstruction process. The second goal is to design a scheme that fits to an anisotropic case. In fact the human body consists of organs which has microscopic structures such as muscle fibers and one may consider it only from macroscopic view. Hence, it is essential to consider it as an anisotropic way. If not, the anisotropic structure of the problem turns into a huge source of instability.

Now we formulate the problem considered in this paper. Let $\Omega \subset \boldsymbol{R}^n$, $n = 2, 3$ be a bounded domain of an electrically conducting body. Let σ be its conductivity distribution. The conductivity distribution $\sigma(\mathbf{x})$ is a positive definite symmetric tensor defined on the domain $\mathbf{x} \in \Omega$. We consider an injection current which is denoted by g. This injection current is applied through a pair of electrodes attached at the boundary. Then, the voltage u satisfies the Maxwell equation with the Neumann boundary condition

$$\begin{aligned} -\nabla \cdot (\sigma \nabla u) &= 0 \quad \text{in} \quad \Omega, \\ -\sigma \nabla u \cdot \nu &= g \qquad \text{on} \quad \partial\Omega, \end{aligned} \tag{1.1}$$

where ν is the outward unit normal vector to the boundary $\partial\Omega$. We assume that the conductivity tensor σ is bounded and strictly positive definite, i.e., there exists positive constants $0 < c_0 < C_0$ such that

$$0 < c_0 \leq \sigma \leq C_0 < \infty \ \text{ in } \ \Omega, \tag{1.2}$$

$$\sigma = \sigma_0 \ \text{ on } \ \partial\Omega. \tag{1.3}$$

where c_0 and C_0 are positive constants and σ_0 is a given tensor on the boundary $\partial\Omega$. It is well known that this Maxwell equation has a unique solution up to an addition by a constant if and only if

$$\int_{\partial\Omega} g dA = 0 \tag{1.4}$$

and hence we always consider a boundary current satisfying this condition. The electrical current $\mathbf{J}$ is given by the relation

$$\mathbf{J} = -\sigma \nabla u.$$

In other words, if the conductivity is given, then the electrical current is uniquely decided for any given boundary injection current.

The inverse problem in this paper is to reconstruct the conductivity σ from the given current data $\mathbf{J}$. Finite element or finite difference methods has been widely used to discretize the conductivity body. In this paper we consider a rectangular resistive network as an approximation of the body. Then the Kirchhoff's voltage law gives a direct method to find the conductivity tensor. First, this method is applied for the isotropic case and the internal conductivity is obtained using one set of current

data $\mathbf{J}$ and a boundary conductivity in two and three space dimension. Then, for the semi-anisotropic conductivity case, that the tensor is given as a diagonal matrix, two sets of current data $\mathbf{J}^1, \mathbf{J}^2$ and the boundary conductivity are used to obtain the conductivity. One can clearly see that the structure of the rectangular resistive network considered in this paper perfectly fits this semi-anisotropic case. It seems that the fully anisotropic case requires a network in a different structure.

One of main interests of the paper is the stability property of the suggested method. The stability of the method is estimated in terms of the condition number of a matrix consists of internal currents. This stability analysis comes from a typical stability analysis of the linear system and we have included it in A. Since the study of conductivity recovery is aiming to recover conductivity of a body such as a human body, the method should be applicable with experimental data which contain experimental noises. Hence, the algorithm should be robust with respect to possible noises to have a practical meaning and we have included various numerical experiments for stability tests.

A large part of this paper is devoted to the numerical simulation of the conductivity recovery focused on the stability test. Let $\mathbf{J}$ be the electrical current without noise. In the stability test we consider a perturbed current $\mathbf{J}^\varepsilon$ with a random noise is given by

$$\mathbf{J}^\varepsilon(x) = (1 + \varepsilon\, \mathbf{R}(x))\mathbf{J}(x), \tag{1.5}$$

where $\mathbf{R}(x)$ is a random noise made by a random number generator which produces values between -1 and 1, and $\varepsilon > 0$ is the measure of the size of the error. In the numerical examples we test the stability of the method with these multiplicative noise. For the isotropic case the noise level has been increased up to $\varepsilon = 40\%$ in Figure 4.2. The method becomes less stable for the semi-anisotropic case and the noise level was increased up to 25% in Figure 4.3. The tests show that three dimensional cases are more stable than two dimensional ones.

The stability of the method also depends on the a-priori estimate in (1.2). In the numerical test the true value of each components of the conductivity tensor is between 1 and 5. Since the exact range of the conductivity should not be assumed in the reconstruction process, we assumed that it is between 0.5 and 10. Hence, if a recovered conductivity value is above 10, then it was set as 10. Similarly, any recovered value below 0.5 was set as 0.5 in the recovery process. It is tested that the method becomes unstable as the range of this a-priori estimate increases.

2. Forward solver based on Kirchhoff's current law.

2.1. Comparison between a network and a finite difference. We start our discussion comparing a finite difference method for the equation (1.1) and a method based on a related resistive network. First, we construct a finite difference scheme in a two dimensional rectangular domain $\Omega = [0, 1] \times [0, 1]$. In this comparison the conductivity distribution is assumed to be isotropic, $\sigma \in \boldsymbol{R}^+$, for a simpler presentation.

The domain Ω is discretized using uniformly distributed meshes

$$x_i = i\Delta x, \quad y_j = j\Delta y, \quad x_{i+1/2} = (i + \frac{1}{2})\Delta x, \quad y_{j+1/2} = (j + \frac{1}{2})\Delta y, \tag{2.1}$$

where $\Delta x = \Delta y = 1/n$ and meaningful subindices are between 0 and n. Consider the four points in Figure 2.1(a):

$$A = (x_{i+1/2}, y_j),\ B = (x_i, y_{j+1/2}),\ C = (x_{i-1/2}, y_j),\ D = (x_i, y_{j-1/2}).$$

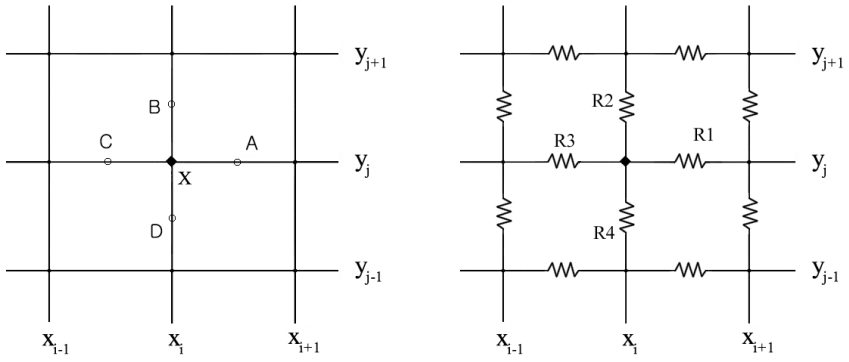

(a) A Finite Difference Mesh (b) A Resistive Network

FIG. 2.1. *A discretization of the finite difference method for a continuous conductivity body and a resistive network provide identical forward solvers.*

Then, the approximation $U_{i,j}$ of the voltage u at the mesh point $X = (x_i, y_j)$ is given by the relation

$$\begin{aligned} &\sigma(A)U_{i+1,j} + \sigma(B)U_{i,j+1} + \sigma(C)U_{i-1,j} + \sigma(D)U_{i,j-1} \\ &\qquad -(\sigma(A) + \sigma(B) + \sigma(C) + \sigma(D))U_{i,j} = 0, \end{aligned} \tag{2.2}$$

which is a typical second order discretization of the equation (1.1). Therefore, if a the conductivity distribution σ and the boundary data g are given, then the approximation of the voltage u can be obtained by solving (2.2) with an appropriate discretization of the Neumann boundary condition. The conductivity σ is usually given at grid points (x_i, y_j)'s and hence the conductivity at the midpoints such as A, B, C and D can be replaced by the average of the conductivity at the adjacent points, e.g., $\sigma(A) \cong \frac{1}{2}[\sigma(x_{i+1}, y_j) + \sigma(x_i, y_j)]$.

Consider a resistive network that discretizes the domain $\Omega = [0,1] \times [0,1]$ as in Figure 2.1(b). The Kirchhoff's current law says that the sum of electrical currents that flow through a given point $X = (x_i, y_j)$ should be zero. Hence, one obtains

$$\frac{1}{R_1}(U_{i+1,j} - U_{i,j}) + \frac{1}{R_2}(U_{i,j+1} - U_{i,j}) + \frac{1}{R_3}(U_{i-1,j} - U_{i,j}) + \frac{1}{R_4}(U_{i,j-1} - U_{i,j}) = 0,$$

where R_i's are resistivity constants of the resistive network in Figure 2.1(b). If it is written in the form of (2.2) for a comparison, then we obtain

$$\frac{1}{R_1}U_{i+1,j} + \frac{1}{R_2}U_{i,j+1} + \frac{1}{R_3}U_{i-1,j} + \frac{1}{R_4}U_{i,j-1} - \Big(\frac{1}{R_1} + \frac{1}{R_2} + \frac{1}{R_3} + \frac{1}{R_4}\Big)U_{i,j} = 0. \tag{2.3}$$

The resistivity is the reciprocal of the conductivity and hence this relation is actually identical to (2.2). The continuous model and the network model for the conductivity body look quite different. However, their discretized models have basically the same structure. Therefore, it is natural to approximate the original continuous conductivity body problem with a resistive network.

If the conductivity tensor σ is given as a diagonal matrix, then the corresponding discretization is almost same as (2.2) after replacing $\sigma(C)$ and $\sigma(D)$ with the first

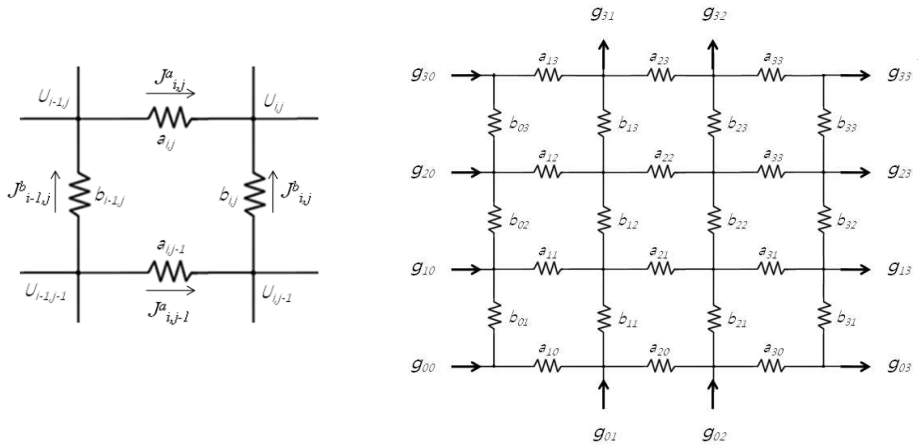

(a) The Kirchhoff's Voltage Law (b) A Resistive Network with $n = 3$

FIG. 2.2. *A continuous conductivity body is discretized using a resistive network. Then the backward solver is given by the Kirchhoff's voltage (or circuit) law.*

and second diagonal elements of the conductivity tensor at the grid point X in Figure 2.1(a), respectively. Hence, the semi-anisotropic case can be easily handled using a network model. It seems that the fully anisotropic case is not covered by the simple structure of the rectangular network in this paper. The fully anisotropic case seems to require a general and a complicate network structure which is beyond the scope of this paper. Therefore, we restrict our study to the isotropic and the semi-anisotropic cases in this paper.

2.2. Algorithm for forward problem. Finding the voltage u or the electrical current $\mathbf{J} = -\sigma\nabla u$ from a given conductivity tensor σ and the normal component of a boundary current $g(x)$, $x \in \partial\Omega$, will be called a forward problem in the followings. We have briefly seen that the Kirchhoff's current law applied to the rectangular resistive network gives a forward solver which is almost identical to the one obtained by a typical finite difference method.

First we introduce the notation for the network. As in Figure 2.2(b), we denote the resistor placed on the left hand side of a grid point (x_i, y_j) by a_{ij} and the one below the grid point by b_{ij}. Then the Kirchhoff's current law related to the grid point (x_i, y_j) is written as

$$\frac{U_{i+1\,j} - U_{ij}}{a_{i+1\,j}} + \frac{U_{i\,j+1} - U_{ij}}{b_{i\,j+1}} + \frac{U_{i-1\,j} - U_{ij}}{a_{i\,j}} + \frac{U_{i\,j-1} - U_{ij}}{b_{i\,j}} = 0,\ 0 \le i, j \le n, \tag{2.4}$$

where the undefined terms on the boundary should be replaced with appropriate input currents (see Figure 2.2(b)), i.e, for $0 \le j \le n$ and $0 < i < n$,

$$\frac{U_{-1\,j} - U_{0j}}{a_{0j}} := g_{0j},\ \frac{U_{n+1\,j} - U_{nj}}{a_{n+1\,j}} := g_{nj},\ \frac{U_{i,-1} - U_{i0}}{b_{i\,0}} := g_{i0},\ \frac{U_{i\,n+1} - U_{in}}{b_{i\,n+1}} := g_{in}. \tag{2.5}$$

Note that there are only three currents related to the four corner points. Hence the four terms excluded are zero, i.e.,

$$\frac{U_{0,-1} - U_{0\,0}}{b_{i\,0}} := \frac{U_{0\,n+1} - U_{0n}}{b_{0\,n+1}} := \frac{U_{n,-1} - U_{nn}}{b_{n\,n+1}} := \frac{U_{n\,n+1} - U_{nn}}{b_{n\,n+1}} := 0. \tag{2.6}$$

In this setting the condition corresponding to $\int_{\partial\Omega} g(x)dx = 0$ is

$$\sum_{j=0}^{n} g_{0j} + \sum_{i=1}^{n-1} g_{i0} = \sum_{j=0}^{n} g_{nj} + \sum_{i=1}^{n-1} g_{in}. \tag{2.7}$$

We have obtained $(n+1)^2$ equations in (2.4) with the same number of unknowns $U_{ij},\ 0 \le i,j \le n$. Hence solving the forward problem implies to solve the system of $(n+1)^2$ equations in (2.4) substituting boundary conditions (2.5) and (2.6) in the place of undefined terms in the system. It is well known that the solution of such a system is unique upto an addition of a constant. Hence we may set $U_{00} = 0$ for the uniqueness. One of the advantages using this network model is the flexibility in handling the boundary data. One may choose the boundary data g_{ij} freely as long as the condition for the boundary data (2.7) is satisfied.

Let J^a_{ij} and J^b_{ij} be the currents that flow the resistors a_{ij} and b_{ij} respectively (see Figure 2.2(a)). Then, they are given by the following relations

$$-J^a_{ij} = (U_{ij} - U_{i-1\,j})/a_{ij}, \qquad -J^b_{ij} = (U_{ij} - U_{i\,j-1})/b_{ij}. \tag{2.8}$$

One may consider $\mathbf{J}_{ij} := (J^a_{ij}, J^b_{ij})$ as the current vector at the mesh point (x_i, y_j).

3. Backward solver in two space dimension. We consider the two dimensional case in this section. Finding the resistivity a_{ij}'s and b_{ij}'s from given electrical currents J^a_{ij}'s and J^b_{ij}'s and boundary resistivity will be called a backward problem in the followings. First note that there are $2n(n+1)$ resistors in the system and $4n$ of them are boundary resistors, which are a_{i0}, a_{in}, b_{0j} and b_{nj} for $1 \le i,j \le n$. We assume that the resistivity of the boundary material can be observed. For our convenience, we assume that $2n$ boundary resistors a_{i0}'s and b_{0j}'s are given and then find the other $2n^2$ unknown resistors including $2n$ boundary resistors a_{in}'s and b_{nj}'s.

Consider a loop given in Figure 2.2(a), where the currents J^a_{ij} and J^b_{ij} flow along the resistors a_{ij} and b_{ij}, respectively. There are n^2 such loops and the Kirchhoff's circuit or voltage law gives n^2 number of equations:

$$J^b_{i-1\,j} b_{i-1\,j} + J^a_{i\,j} a_{i\,j} - J^b_{i\,j} b_{i\,j} - J^a_{i\,j-1} a_{i\,j-1} = 0, \qquad 1 \le i,j \le n. \tag{3.1}$$

Therefore, it is clear that one set of current data is not enough to solve this backward problem and we use two or more current data. However, if an isotropic conductivity is considered, the single set of current data is just enough and we will see it in the following section.

There are four unknowns in the equation (3.1). Since we assume that the resistivity is known on the boundary we may assume that two of them are known if the loop under consideration is at one of the four corners. If we have two data sets for the currents, then we can solve (3.1) at the corner loop. We may continue this process since one can find a loop that two of the resistors are known until all of them are computed. Note that, if a current vector is given at a grid point (x_i, y_j), then we may set its x and y components as J^a_{ij} and J^b_{ij} respectively.

3.1. Isotropic conductivity in two dimensional space. The conductivity tensor product is actually a scalar multiplication in an isotropic case. For the two dimensional case we may simply set $a_{ij} = b_{ij}$ and consider a_{ij} as this isotropic resistivity value at the grid point (x_i, y_j). Then there are basically n^2 unknowns left since

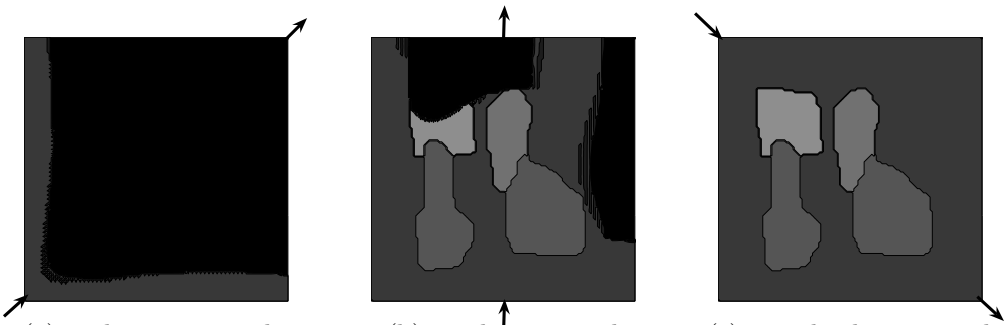

(a) nothing recovered (b) partly recovered (c) completely recovered

FIG. 3.1. *Two dimensional isotropic conductivity has been recovered under three different injection currents. Injection currents are denoted by arrows. The best result is (c). In this example noise levels are all zero.*

the boundary resistors on the x, y-axes are given. Hence the resistivity can be recovered using a single data set of currents. Suppose that $a_{i-1\,j}$ and $a_{i\,j-1}$ are already obtained in the previous steps. Then a_{ij} is obtained by

$$a_{ij} = \frac{J^a_{i\,j-1}}{J^a_{i\,j} - J^b_{i\,j}}\, a_{i\,j-1} - \frac{J^b_{i-1\,j}}{J^a_{i\,j} - J^b_{i\,j}}\, a_{i-1\,j}\,. \tag{3.2}$$

This means that the isotropic conductivity can be obtained if $J^a_{i\,j} - J^b_{i\,j} \neq 0$ for all i's and j's. It is shown that two sets of current data are required to obtain the uniqueness of conductivity recovery in [14]. Note that we have assumed that the conductivity is given on the boundary and hence the non-uniqueness phenomena is not observed.

It is clear that, if $J^a_{i\,j} - J^b_{i\,j}$ is close to zero, then it is hard to get the conductivity recovered since it is the denominator in the conductivity reconstruction algorithm formula in (3.2). Hence it is important to consider a injection current to avoid such a situation. First consider the worst the injection current that uses two corner points $(0, 0)$ and $(1, 1)$ (i.e., $g_{00} = g_{nn} = 1$ and all the other boundary currents are zero). Then the main stream of the current is in the direction of vector $(1, 1)$ which will make the denominator in (3.2) be small. In Figure 3.1(a) the results of recovered conductivity is given using this injection current. Even though the numerical computation has been done under very small noise, the conductivity is not recovered at all.

If the current is injected using the points $(0.5, 0)$ and $(0.5, 1)$ as in Figure 3.1(b), some portion of the conductivity is recovered. However, there are spots that the results are poor. It seems that the bad spots start from a point that the electric current becomes parallel to the vector $(1, 1)$. The best case is the one that the current is injected using the points $(1, 0)$ and $(0, 1)$. Then the main stream of the current is aligned to the direction of slope negative one and $J^a_{i\,j} - J^b_{i\,j}$ seems not be close to zero. The recovered conductivity is given in Figure 3.1(c) which shows perfect recovered image. Note that these images were recovered without noise.

In the following two dimensional isotropic examples we apply an injection current same as the case (c). The reason for this preferred direction of current is due to the assumption $a_{ij} = b_{ij}$. If the injection current in Figure 3.1(a) should be employed, then we may consider the model under the assumption that $a_{ij} = b_{i-1\,j}$. Then, under this assumption, we may obtain the conductivity correctly. It is also possible

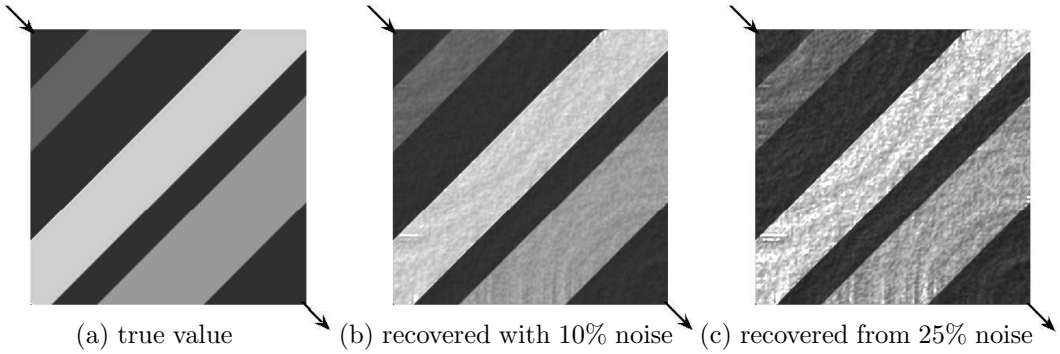

(a) true value (b) recovered with 10% noise (c) recovered from 25% noise

FIG. 3.2. *This is an example that the discontinuity of the conductivity is orthogonal to the main stream of the current. Since the boundary conductivity is assumed to be given, the conductivity is reasonably recovered even with 25% of noise.*

to recover the conductivity after dividing the whole domain into several parts. Then, the image of each part of the domain can be computed starting from a corner point and then combined to get the whole picture. For simplicity, we consider the model case $a_{ij} = b_{ij}$ only for the isotropic case and the injecting current given as in Figure 3.1(c) in the following numerical examples.

REMARK 3.1. *Notice that under the assumption $a_{ij} = b_{ij}$ for the isotropic case there is a preferred direction of current injection. This non-symmetric structure of the scheme can be neutralized as in the followings. Let r_{ij} be the resistivity at the grid point (x_i, y_j). Then, the resistivity a_{ij} and b_{ij} can be replaced as the average of the adjacent resistivity, i.e., (3.1) can be replaced by*

$$J^b_{i-1\,j}\frac{r_{i-1,j}+r_{i-1,j-1}}{2}+J^a_{ij}\frac{r_{ij}+r_{i-1,j}}{2}-J^b_{ij}\frac{r_{ij}+r_{i,j-1}}{2}-J^a_{i\,j-1}\frac{r_{ij-1}+r_{i-1,j-1}}{2}=0.$$

Suppose that $r_{i-1\,j}, r_{i\,j-1}$ and $r_{i-1\,j-1}$ are already obtained in the previous steps. Then r_{ij} is obtained by

$$r_{ij}=\frac{J^a_{i\,j-1}(r_{ij-1}+r_{i-1,j-1})-J^b_{i-1\,j}(r_{i-1,j}+r_{i-1,j-1})}{J^a_{i\,j}-J^b_{i\,j}}+J^b_{ij}r_{i,j-1}-J^a_{ij}r_{i-1,j}.$$

Hence we still need to have the same denominator $J^a_{i\,j}-J^b_{i\,j}$ to be large enough to have stability. Furthermore the extra addition term $J^b_{ij}r_{i,j-1}-J^a_{ij}r_{i-1,j}$ is another source of noise which is proportional to $(J^b_{ij}-J^a_{ij})$. Hence this scheme is more sensitive on the noise and the numerical examples show blowups for small noise size. The advantage of this method is that one may use it as increasing or decreasing the indexes due to the symmetry of the structure. However, we did not use this form due to its noise sensitivity.

Note that the boundary resistivity is assumed to be given. This assumption makes it possible to obtain the isotropic conductivity using a single set of data. It is well known that if the electrical current is perpendicular to the discontinuity curve of the conductivity, then such a change is not detectible. In Figure 3.2 such a case is tested. Even the case with 25% noise the conductivity is recovered reasonably. It is pretty obvious that the given boundary resistivity makes the problem stable. However, one may still find some traces of equipotential lines from the last image with 25% noise.

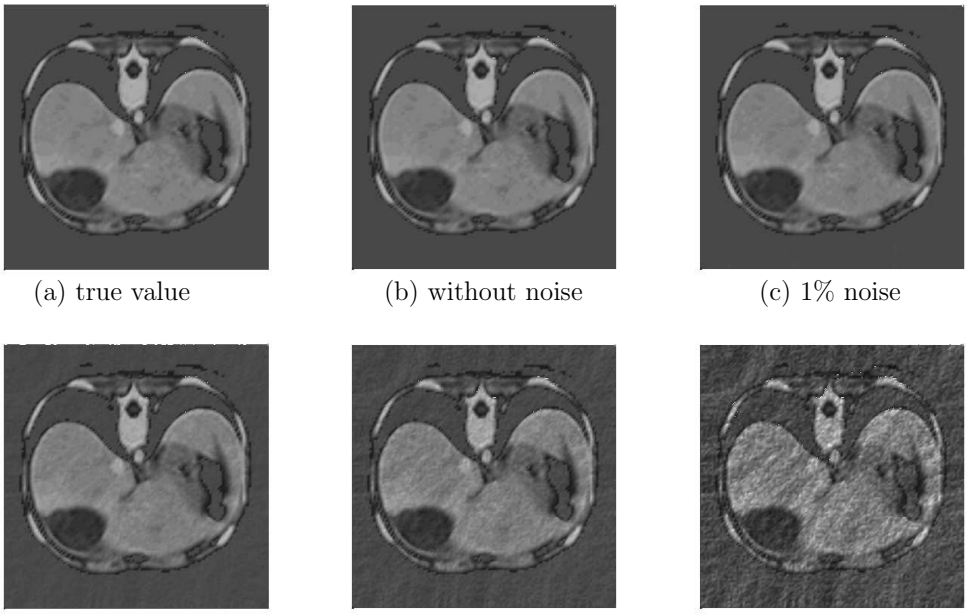

(a) true value (b) without noise (c) 1% noise

(d) 5% noise (e) 10% noise (f) 25% noise

FIG. 3.3. *Isotropic conductivity recovery in two dimensional space. The noise level is increased up to 25%.*

In Figure 3.3, a numerical example using a CT image of a human body is given. It is possible that certain geometric structure of the body may trigger a singularity property of the method. In this example one may observe that even if the noise level is of 25% the two dimensional conductivity is recovered reasonably. This level of stability is of satisfactory and seems to have better stability property than most of other methods. However, one may observe a singularity from the with a noise level higher than this that starts from the point (x_{20}, y_{45}) (see the third figure in the second row of Figure 4.2).

3.2. Two dimensional semi-anisotropic conductivity. If the conductivity tensor is a diagonal matrix, which is called a semi-anisotropic case in this paper, the diagonal elements correspond to a_{ij} and b_{ij} for the two dimensional case. If the diagonal entries are any positive numbers, then the tensor is positive definite. Hence, we may take any two images as vertical and horizontal resistors a_{ij}'s and b_{ij}'s respectively. The total number of resistors for the two dimensional resistive network is $2n^2 + 2n$. If $2n$ boundary resistors a_{i0}'s and b_{0j}'s are given, then $2n^2$ unknown resistors are left. Since the Kirchhoff's circuit law gives n^2 number of equations as in (3.1), it is clear that one set of current data is not enough for the solvability. We should employ at least two sets of current data and we denote them by J_{ij}^{ka} and J_{ij}^{kb}, $k = 1, 2$. Then we obtain $2n^2$ equations:

$$\begin{aligned} J_{i\,j}^{1a} a_{i\,j} - J_{i\,j}^{1b} b_{i\,j} &= J_{i\,j-1}^{1a} a_{i\,j-1} - J_{i-1\,j}^{1b} b_{i-1\,j}, \\ J_{i\,j}^{2a} a_{i\,j} - J_{i\,j}^{2b} b_{i\,j} &= J_{i\,j-1}^{2a} a_{i\,j-1} - J_{i-1\,j}^{2b} b_{i-1\,j}, \end{aligned} \qquad 1 \le i, j \le n. \tag{3.3}$$

Suppose that a_{ij-1} and b_{i-1j} are boundary resistors or obtained from previous

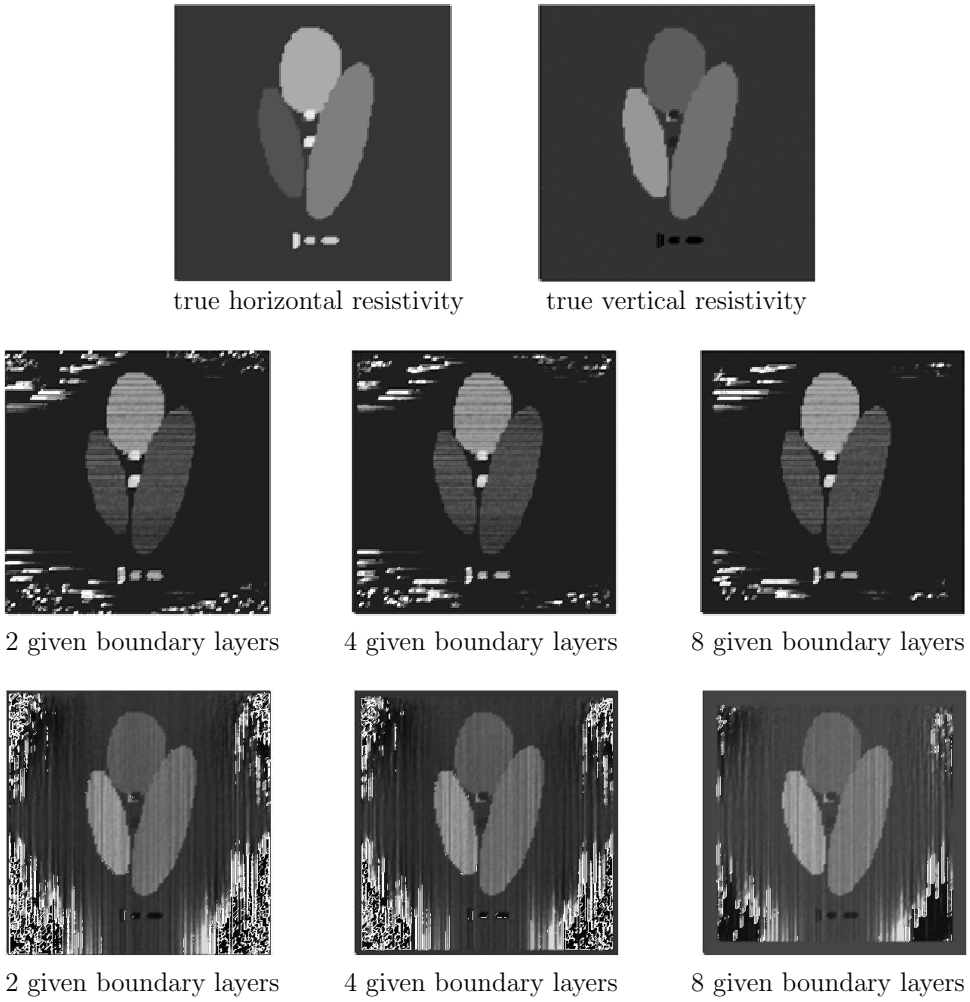

FIG. 3.4. *Two dimensional semi-isotropic conductivity images obtained as increasing the number of given boundary layers from 2 to 8. The noise level is 5%. The images in the second row are of horizontal resisters a_{ij}'s and the ones in the third row are for b_{ij}'s.*

steps. Then a_{ij} and b_{ij} can be computed by solving the 2 by 2 system in (3.3). Therefore, the stability of the method depends on the condition number of the matrix

$$A = \begin{pmatrix} J_{ij}^{1a} & J_{ij}^{1b} \\ J_{ij}^{2a} & J_{ij}^{2b} \end{pmatrix}. \tag{3.4}$$

From the numerical examples for the isotropic case one observes that the direction of injection currents should be perpendicular to the vector $(1, 1)$. Unlike the isotropic case the direction of each injecting current does not make a difference since $a_{ij} = b_{ij}$ is not assumed in this anisotropic case. However, if the two currents $\mathbf{J}^1$ and $\mathbf{J}^2$ become parallel at a point, the matrix becomes singular. Hence, it is required to reduce the condition number of the matrix A by making the two currents vectors have large anlges. In the followings we consider two methods.

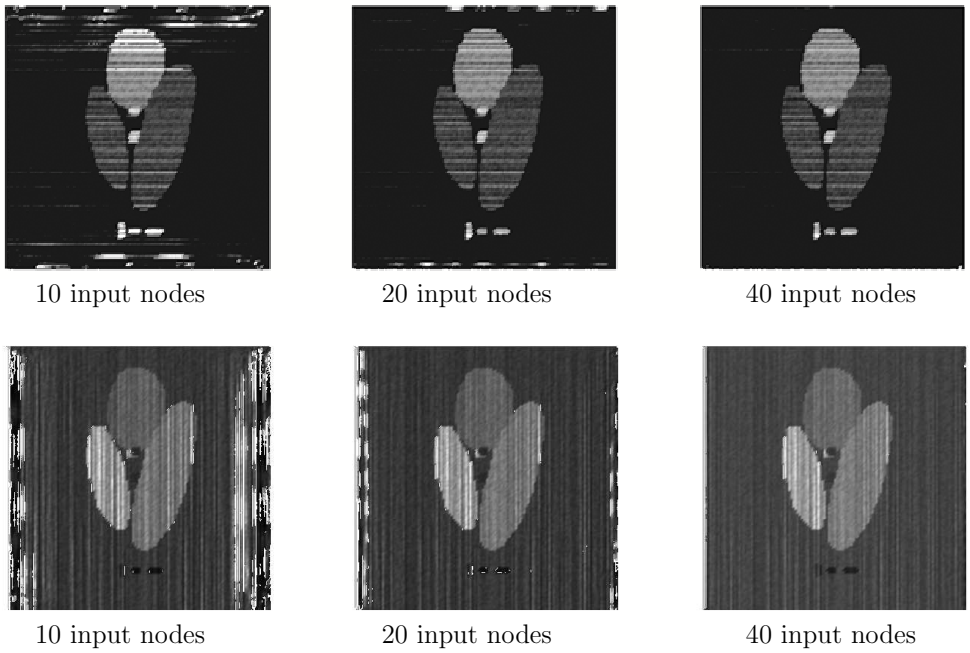

FIG. 3.5. *Two dimensional semi-isotropic conductivity images obtained as increasing the number of input nodes from 10 to 40. For example, five input nodes were used to each of two parallel sides which totals ten input nodes. The noise level in this example is 10%.*

First, notice that the electrical current becomes parallel to the boundary if it is away from the boundary current sources. This makes the matrix in (3.4) have large condition numbers along the boundary. To reduce this boundary effect the resistors in several boundary layers are assumed to be given. It is tested as increasing the number of given layers in Figure 3.4. The recovered conductivity images show interesting behavior. The conductivity image near the boundary is very poor, which was expected due to the condition number of the matrix A. Since the reconstruction technique is performed from the boundary cells, the interior image can be affected by this poor boundary image. However, the inside image is better than the boundary one. It seems that there is a mechanism that neutralizes the boundary blowups. Another interesting phenomenon is that, even if several boundary layers are given, it does not make significant changes. An interesting thing is that the images of horizontal resistors a_{ij} in the second row of Figure 3.4 show horizontal strips and the images for b_{ij}'s show vertical strips. One may also find similar phenomenon in the three dimensional computations, Figures 4.3 and 4.4. However, the trips are weaker in the three dimensional examples.

The second approach is to increase the number of input nodes. So far we have used only two nodes, which is an extreme case. Now we increase the number of nodes up to forty. Note that one of the main advantages of using a resistive network method is that the input current $g(x)$, $x \in \partial\Omega$, is not required in the reconstruction process. Hence one may choose even a random input data using various number of nodes at various places for input currents as long as (2.5) is satisfied. This property removes many annoying experimental concerns if one uses a reconstruction method depending

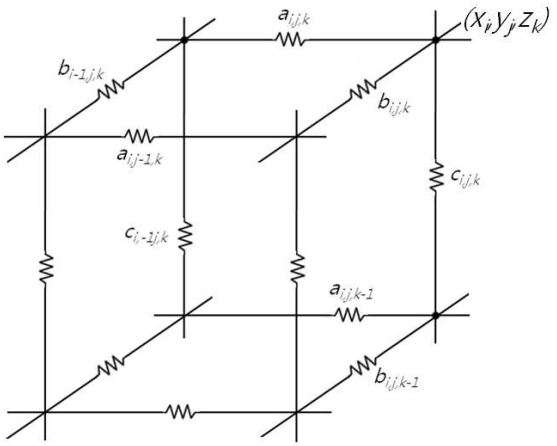

FIG. 4.1. *A cell of a three dimensional resistive Network*

on the boundary input data. In Figure 3.5 conductivity images are recovered as increasing the number of input nodes. One may observe that the method becomes more stable as the number of input nodes are increased.

In these examples one may observe that the semi-anisotropic case is more unstable in compare with the isotropic one. For the isotropic case the conductivity image has been recovered using only two input nodes with an acceptable resolution even with the noise level 25%. However, the images for the semi-anisotropic case is very poor under the same conditions.

4. Backward solver in three space dimension. We now consider the three dimensional case. A cell for a three dimensional resistive network is given in Figure 4.1. First note that there are $3n(n+1)^2$ resistors in the system and $12n^2$ of them are boundary ones. Since the conductivity of the boundary material can be observed, the unknown resistors are $3n(n-1)^2$ interior ones. For our convenience, we assume that boundary resistors on the xy-,xz- and yz-planes are given. Then $3n^3$ resistors left which will be decided by the reconstruction method.

Consider the three faces of the cubic cell in Figure 4.1 that contains the vertex (x_i, y_j, z_k). If the Kirchhoff's circuit law is applied to each of these three faces, then we obtain

$$\begin{aligned} &J^a_{ijk}a_{ijk} - J^b_{ijk}b_{ijk} = J^a_{i\,j-1\,k}a_{i\,j-1\,k} - J^b_{i-1\,jk}b_{i-1\,jk}, \\ &J^b_{ijk}b_{ijk} - J^c_{ijk}c_{ijk} = J^b_{ij\,k-1}b_{ij\,k-1} - J^c_{i\,j-1\,k}c_{i\,j-1\,k}, \qquad 1 \le i,j,k \le n. \\ &J^a_{ijk}a_{ijk} - J^c_{ijk}c_{ijk} = J^a_{ij\,k-1}a_{ij\,k-1} - J^c_{i-1\,jk}c_{i-1\,jk}, \end{aligned} \tag{4.1}$$

Suppose that the resistors with subindexes other than '$_{ijk}$' are given in previous steps. Then the right hand sides are given terms, and the three unknown resistors with subindex '$_{ijk}$' should be computed using these three equations. Adding first two equations gives

$$J^a_{ijk}a_{ijk} - J^c_{ijk}c_{ijk} = J^a_{i\,j-1\,k}a_{i\,j-1\,k} + J^b_{ij\,k-1}b_{ij\,k-1} - J^c_{i\,j-1\,k}c_{i\,j-1\,k} - J^b_{i-1\,jk}b_{i-1\,jk}.$$

Comparing this equation to the third one in (4.1), one can easily see that the linear system has a solution only if

$$J^a_{i\,j-1\,k}a_{i\,j-1\,k} - J^a_{ij\,k-1}a_{ij\,k-1} + J^b_{ij\,k-1}b_{ij\,k-1} - J^b_{i-1\,jk}b_{i-1\,jk}J^c_{i-1\,jk}c_{i-1\,jk} - J^c_{i\,j-1\,k}c_{i\,j-1\,k} = 0.$$

Then, the third equation in (4.1) is the sum of the first two. Hence, we have obtained only two equations applying the Kirchhoff's circuit law to the three dimensional cell. There are $2n^3$ equations in total, which are enough for the isotropic cases but not for semi-anisotropic cases.

4.1. Isotropic case. For the three dimensional case we similarly set $a_{ijk} = b_{ijk} = c_{ijk}$ and consider a_{ijk} as the isotropic conductivity value at the grid point (x_i, y_j, z_k). Then the problem becomes over determined. Hence we should consider a way that maximizes the information. We rewrite (4.1) as

$$\begin{aligned} a_{ijk} &= (J^a_{i\,j-1\,k} a_{i\,j-1\,k} - J^b_{i-1\,jk} a_{i-1\,jk})/(J^a_{ijk} - J^b_{ijk}), \\ a_{ijk} &= (J^c_{i-1\,jk} a_{i-1\,jk} - J^a_{ij\,k-1} a_{ij\,k-1})/(J^a_{ijk} - J^c_{ijk}), \\ a_{ijk} &= (J^b_{ij\,k-1} a_{ij\,k-1} - J^c_{i\,j-1\,k} a_{i\,j-1\,k})/(J^b_{ijk} - J^c_{ijk}), \end{aligned} \qquad 1 \le i, j, k \le n. \tag{4.2}$$

Therefore, if $J^a_{ijk} = J^b_{ijk} = J^c_{ijk}$, the problem is unsolvable. If the three terms are close to each other, then the recovery of the conductivity becomes unstable to noises. Hence we need to avoid such a situation to obtain a stable conductivity recovery.

The first strategy is to choose one of the three equations that makes the method most stable. Consider three quantities

$$A := \frac{J^a_{ijk} + J^b_{ijk}}{\sqrt{(J^a_{ijk})^2 + (J^b_{ijk})^2}}, \quad B := \frac{J^a_{ijk} + J^c_{ijk}}{\sqrt{(J^a_{ijk})^2 + (J^c_{ijk})^2}}, \quad C := \frac{J^b_{ijk} + J^c_{ijk}}{\sqrt{(J^b_{ijk})^2 + (J^c_{ijk})^2}}.$$

These measure the cosine of the angle between vectors $(1,1)$ and (J^a_{ijk}, J^b_{ijk}), (J^a_{ijk}, J^c_{ijk}) or (J^b_{ijk}, J^c_{ijk}), respectively. Hence we choose the equation corresponding to the smallest one.

The second strategy is to choose an injection current in a way that the main stream of the electric current is orthogonal to the diagonal direction vector $\mathbf{v}_1 = (1,1,1)/\sqrt{3}$. For a comparison purpose we consider three kinds of injection currents. For the first injection current we chose two points $(0,0,0)$ and $(1,1,1)$. Then the main current direction is parallel to $\mathbf{v}_1$, which should be the worst case. In the first row of Figure 4.2 conductivity images recovered using this current are given. This numerical computation has been done for a three dimensional case with $128 \times 128 \times 128$ mesh and then the slice which is identical to the two dimensional image has been displayed. In this case the image is recovered without noise only. Note that two dimensional conductivity is not recovered at all even without noise, Figure 3.1(a). The three dimensional case has more stability than the two dimensional one.

The second injection current is given through two vertex points $(1,0,1)$ and $(0,1,0)$. Let $\mathbf{v}_2$ be the unit vector that connects these two points, i.e., $\mathbf{v}_2 = (1,-1,1)/\sqrt{3}$. The angle between the vectors $\mathbf{v}_1$ and $\mathbf{v}_2$ is given by

$$\cos\theta = \mathbf{v}_1 \cdot \mathbf{v}_2 = 1/3,$$

i.e., the angle is about 70.5 degree. In the second rwo of Figure 4.2 conductivity images recovered using this current are given. In this case the conductivity is well recovered even with high noise levels. In compare with Figure 3.1(b) this three dimensional case is more stable on noises than the two dimensional case. Note that, under the noise level of 40%, there is a black strip in the middle of the left half.

The last injection current uses two middle points of edges, $(0,1,0.5)$ and $(1,0,0.5)$. Let $\mathbf{v}_3$ be the unit vector that connects these two points, i.e., $\mathbf{v}_3 = (1,-1,0)/\sqrt{2}$. This

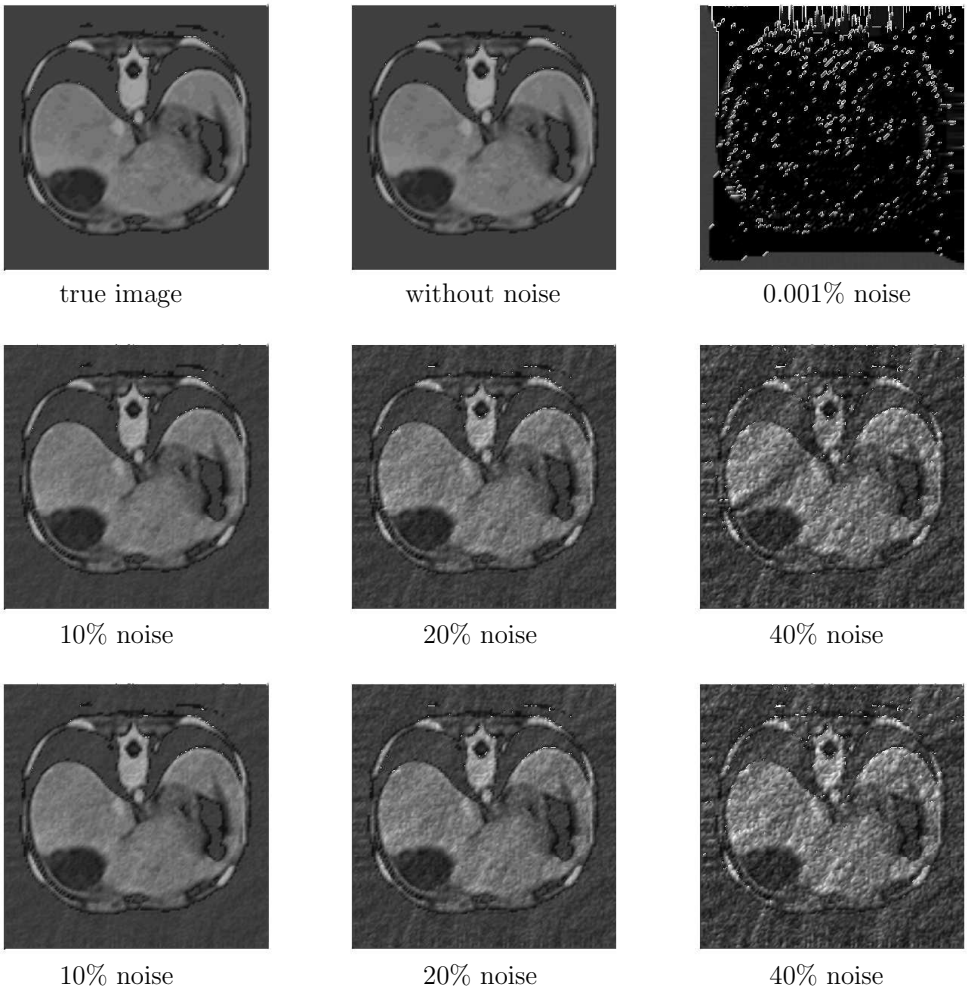

FIG. 4.2. *Isotropic conductivity image in three dimension. Injection current for the first row is given through two points* $(0,0,0)$ *and* $(1,1,1)$. *The second row uses* $(1,0,1)$ *and* $(0,1,0)$ *and the third one uses* $(0,1,0.5)$ *and* $(1,0,0.5)$.

vector is orthogonal to the diagonal direction, i.e.,

$$\cos\theta = \mathbf{v}_1 \cdot \mathbf{v}_3 = 0.$$

In the third row of Figure 4.2 three images recovered using this injection current are given. The recovered images are better than the ones in the second row. In particular the one of noise level of 40% does not have a black strip in this case.

4.2. Anisotropic case. It is clear that one set of current data is not enough to decide a_{ijk}'s, b_{ijk}'s and c_{ijk}'s and hence we use two data sets for the backward solver.

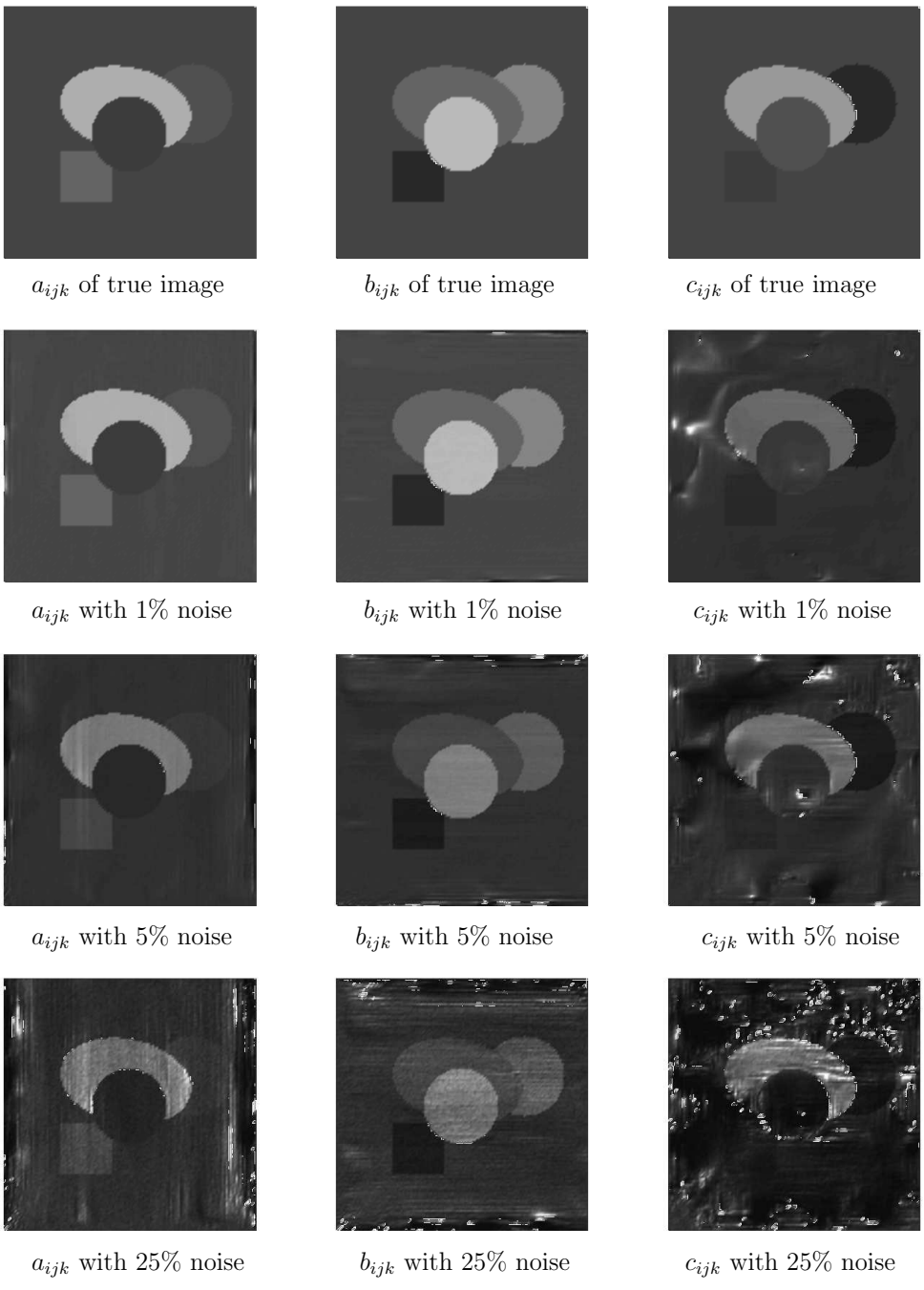

FIG. 4.3. *Three dimensional semi-anisotropic conductivity images. Two sets of injection currents are applied in the direction of x and y-axes. These figures are slices of three dimensional body orthogonal to the z-axis with* $k = 68$ *out of* 128. *The image for* c_{ijk} *is worse than others since the current in the direction is weaker.*

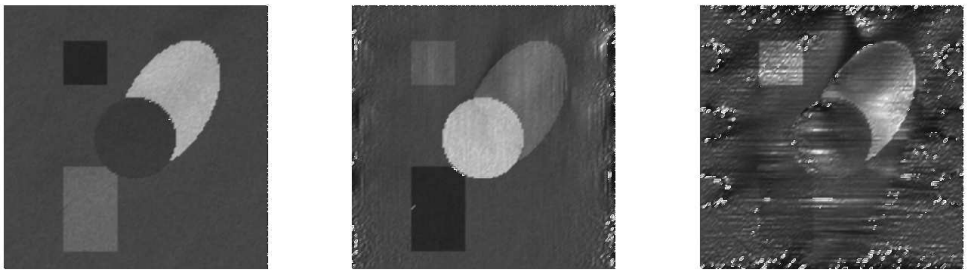

Images for a_{ijk}, b_{ijk} and c_{ijk} reconstructed under a-priori estimate: $0.5 \le \sigma \le 10$.

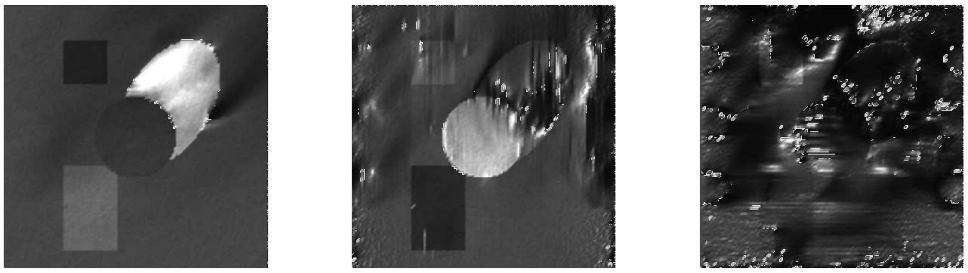

Images for a_{ijk}, b_{ijk} and c_{ijk} reconstructed under a-priori estimate: $0.25 \le \sigma \le 20$.

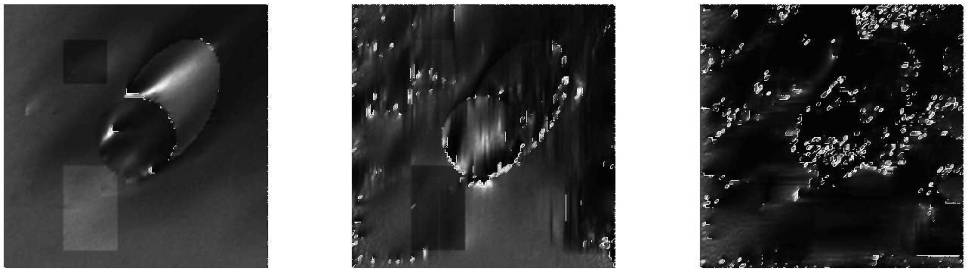

Images for a_{ijk}, b_{ijk} and c_{ijk} reconstructed under a-priori estimate: $0.125 \le \sigma \le 40$.

FIG. 4.4. *Three dimensional semi-anisotropic conductivity images. Two sets of injection currents are applied in the direction of x and y-axes. These figures are slices of three dimensional body orthogonal to the x-axis with* $i = 60$ *out of* 128 *layers. The actual conductivity is range is* $1 \le \sigma \le 5$. *The noise level of this example is* 10%.

Let $\mathbf{J}^1$ and $\mathbf{J}^2$ be the given currents. Then the Kirchhoff's circuit law gives

$$\begin{aligned}
J^{1a}_{ijk} a_{ijk} - J^{1b}_{ijk} b_{ijk} &= J^{1a}_{i\,j-1\,k} a_{i\,j-1\,k} - J^{1b}_{i-1\,jk} b_{i-1\,jk},\\
J^{1b}_{ijk} b_{ijk} - J^{1c}_{ijk} c_{ijk} &= J^{1b}_{ij\,k-1} b_{ij\,k-1} - J^{1c}_{i\,j-1\,k} c_{i\,j-1\,k},\\
J^{2a}_{ijk} a_{ijk} - J^{2b}_{ijk} b_{ijk} &= J^{2a}_{i\,j-1\,k} a_{i\,j-1\,k} - J^{2b}_{i-1\,jk} b_{i-1\,jk},\\
J^{2b}_{ijk} b_{ijk} - J^{2c}_{ijk} c_{ijk} &= J^{2b}_{ij\,k-1} b_{ij\,k-1} - J^{2c}_{i\,j-1\,k} c_{i\,j-1\,k},
\end{aligned} \qquad 1 \le i, j, k \le n. \tag{4.3}$$

In Figure 4.3 a numerical experiment for three dimensional semi-anisotropic conductivity reconstruction is given. First, for this experiment, a three dimensional cubic domain $\Omega = [0,1]^3$ is discretized into 128^3 cubic cells and three dimensional images have been constructed for resisters a_{ijk}'s, b_{ijk}'s and c_{ijk}'s. For the current injections, two kinds of injection currents are applied using 20 input nodes. The first set of electrical current data is measured after applying the boundary current on two sides

which are parallel to the yz-plan. The second one is measured after applying the currents on the sides parallel to xy-plan. Note that these two currents are mostly move to the direction of x and y axes. Hence z-component of the current is weaker than others.

The images for a_{ijk}'s and b_{ijk}'s in Figure 4.3 are in a good shape. However, the one for c_{ijk}'s is poor. Hence it needs to make the current move to the direction of z-axis to obtain the conductivity image related to the direction. The images for a_{ijk}'s and b_{ijk}'s are in a pretty good shape even with 25% noise. There are lines in the images which is weaker than the ones of the two dimensional cases. Hence, it seems that the three dimensional case is more stable that the two dimensional one.

In this example the true conductivity is in the range between 1 and 5. In the construction process, it is assumed that we have an a-priori estimate that conductivity satisfies $0.5 \leq \sigma \leq 10$. Hence any reconstructed conductivity value higher than 10 was set as 10. Similarly, any value below 0.5 was set as 0.5. In Figure 4.4, the performance is tested under a different a-priori estimates. The first row of the figure is simply a different slice of the previous example which uses the same a-priori estimate $0.5 \leq \sigma \leq 10$. The images in the second and third rows were built using a-priori estimates $0.25 \leq \sigma \leq 20$ and $0.125 \leq \sigma \leq 40$, respectively. In the figures one can clearly observe that the performance of the method strongly depends on the a-priori estimate of the conductivity.

5. Conclusions. A conductivity reconstruction method based on a rectangular resistive network is suggested for two and three dimensional spaces. This method handles both of isotropic and semi-anisotropic cases. For the stability test a multiplicative random noise has been added and numerical examples show stable behavior of the method. Three dimensional examples are more stable than the two dimensional ones. The noise level can be increased up to 40% for three dimensional isotropic case. For the three dimensional semi-anisotropic case is done up to 25% noise level. Since this is a direct method based on the Kirchhoff's laws of current and voltage, the computation time is minimum. It take about couple of minutes for the three dimensional case with 128^3 meshes with a personal computer.

There are several things that should be done to complete the project. A network with a general structure should be introduced to handle general anisotropic cases. We could not handle them with the rectangular network in this paper. A noise reducing technique should be developed that fits with resistive networks. In this paper we have tested how the method works under noise. The final goal of this project is to obtain the real conductivity of a human body. Hence one should work with experimental data and understand the noise and its effect to the method.

There are also remaining questions raised by this work. We could reconstruct the conductivity using a single set of internal current if the boundary conductivity is given. For semi-anisotropic cases two sets were required both of two and three space dimensions. Considering the number of unknowns and equations, it seems to require three sets of internal currents both of two and three dimensional anisotropic cases. Mathematically we do not have answers on this question. One may observe from Figure 3.4 that the interior conductivity is recovered well even if there are severe oscillations near the boundary. Furthermore, the recovered conductivity images of semi-anisotropic cases have vertical and horizontal lines. It needs to understand these behaviors of the method to obtain better results.

Appendix A. Stability analysis. In this section we consider the stability of the conductivity reconstruction method based on a resistive network. For simplicity, we consider a two dimensional object with semi-anisotropic conductivity. The total number of resistors for such a case is $2n^2+2n$. The $2n$ boundary resistors, a_{i0}'s and b_{0j}'s, are assumed to be given. Hence the number of unknown resistors is $2n^2$. If the currents J^a_{ij}, J^b_{ij} that flow through the resistors a_{ij} and b_{ij}, respectively, are given for all $0 \le i,j \le n$, then the Kirchhoff's circuit law gives n^2 number of equations as in (3.1). In the numerical examples two or more sets of current data can be used. In doing that two equations has been chosen in the way that the corresponding 2×2 matrix has the smallest condition number among other possible choices.

In the followings we consider the currents which are chosen in a way that the following matrix

$$A = \begin{pmatrix} J^{1a}_{ij} & J^{1b}_{ij} \\ J^{2a}_{ij} & J^{2b}_{ij} \end{pmatrix}$$

is not singular and has the smallest condition number among other possible choices. Then we solve the following $2n^2$ equations

$$\begin{aligned} &J^{1a}_{i\,j}a_{i\,j} - J^{1b}_{i\,j}b_{i\,j} + J^{1b}_{i-1\,j}b_{i-1\,j} - J^{1a}_{i\,j-1}a_{i\,j-1} = 0, \\ &J^{2a}_{i\,j}a_{i\,j} - J^{2b}_{i\,j}b_{i\,j} + J^{2b}_{i-1\,j}b_{i-1\,j} - J^{2a}_{i\,j-1}a_{i\,j-1} = 0, \end{aligned} \qquad 1 \le i,j \le n. \tag{A.1}$$

Since a_{i0}'s and b_{0j}'s are given, these $2n^2$ equations can be written as

$$C\mathbf{x} = \mathbf{f}, \tag{A.2}$$

where $C=(c_{ij})$ is a $2n^2\times 2n^2$ sparse matrix consists of the coefficients $J^{1a}_{ij}, J^{1b}_{ij}, J^{2a}_{ij}$ and J^{2b}_{ij} and the vector $\mathbf{x}$ is $2n^2$ column vector consists of $2n^2$ unknown resistors. The right hand side column vector $\mathbf{f}$ appears due to the given boundary resistor and hence it has at most $2n-1$ nonzero elements.

For the stability analysis consider perturbed current data $\tilde{\mathbf{J}}^k_{ij}$'s with noise. Then the linear system one may obtain is an approximation of the exact one (A.2) that is written as

$$\tilde{C}\tilde{\mathbf{x}} = \tilde{\mathbf{f}}. \tag{A.3}$$

Now we test the stability of the problem. Let

$$\mathbf{e} = \tilde{\mathbf{x}} - \mathbf{x}, \quad E = \tilde{C} - C, \quad \mathbf{h} = \tilde{\mathbf{f}} - \mathbf{f} \ \text{ and } \ \mathbf{H}^k_{ij} = \tilde{\mathbf{J}}^k_{ij} - \mathbf{J}^k_{ij}, \quad 0 \le i,j \le n,\ k = 1,2.$$

The condition number of a nonsingular matrix C is $\kappa = \mathrm{cond}(C) = \|C\|_\infty \|C^{-1}\|_\infty$. Let $\rho(C)$ be the smallest eigenvalue of the matrix C. First we consider the solvability of the perturbed problem which depends on the following lemma:

Neumann Lemma *If $\rho(C^{-1}E) \le \|C^{-1}\|_\infty \cdot \|E\|_\infty < 1$, then $I + C^{-1}E$ is invertible. Hence $C(I+C^{-1}E) = C + E = \tilde{C}$ is invertible, too.*

One can easily see that $E = \tilde{C} - C$ has at most four nonzero elements in each row, it is clear that

$$\begin{aligned} \|E\|_\infty &= \max_{1\le i\le 2n^2} \Big(\sum_{j=1}^{2n^2} |e_{ij}| \Big) \le 4 \max_{0\le i,j\le n} (|H^{1a}_{ij}|, |H^{1b}_{ij}|, |H^{2a}_{ij}|, |H^{2b}_{ij}|), \\ \|\mathbf{h}\|_\infty &= \max_{1\le i\le 2n^2} |h_i| \le \max_{0\le i,j\le n} (|a_{i0}H^{1a}_{i0}|, |b_{0j}H^{1b}_{0j}|, a_{i0}|H^{2a}_{i0}|, b_{0j}|H^{2b}_{0j}|). \end{aligned} \tag{A.4}$$

Hence, if

$$\max_{0\le i,j\le n}(|H_{ij}^{1a}|,|H_{ij}^{1b}|,|H_{ij}^{2a}|,|H_{ij}^{2b}|) < \frac{1}{4\|C^{-1}\|_\infty} = \frac{\|C\|_\infty}{4\kappa}, \tag{A.5}$$

the perturbed problem (A.3) is solvable.

Using (A.2) the perturbed system can be written as

$$(C+E)\mathbf{e} = \mathbf{h} - E\mathbf{x},$$

and

$$\mathbf{e} = (C+E)^{-1}(\mathbf{h}-E\mathbf{x}) = (I+C^{-1}E)^{-1}C^{-1}(\mathbf{h}-E\mathbf{x}).$$

Hence the error $\mathbf{e} = \tilde{\mathbf{x}} - \mathbf{x}$ is estimated by

$$\|\mathbf{e}\|_\infty \le \frac{\|C^{-1}\|_\infty}{1-\|C^{-1}E\|_\infty}(\|\mathbf{h}\|_\infty + \|E\|_\infty\|\mathbf{x}\|_\infty).$$

Since the exact solution $\mathbf{x}$ is bounded and E and $\mathbf{h}$ are bounded by (A.4), the error is estimated by

$$\|\mathbf{e}\|_\infty \le \frac{\|C^{-1}\|_\infty}{1-\|C^{-1}E\|_\infty}[1+4R\max_{0\le i,j\le n}(|H_{ij}^{1a}|,|H_{ij}^{1b}|,|H_{ij}^{2a}|,|H_{ij}^{2b}|)\,], \tag{A.6}$$

where R is the maximum resistor. Hence the error $\mathbf{e}$ decays to zero as the noises of the current data converge to zero. Therefore, under the stability condition (A.5), the approximation error of the method is estimated by (A.6).

Acknowledgment. The authors would like to thank Professor Hyea-Hyun Kim. She kindly helped authors in developing numerical schemes for a forward solver in the early stage of this project and gave them valuable advices.

REFERENCES

[1] G. Alessandrini, Examples of instability in inverse boundary value problems, Inverse Problems, 13 (1997), 887–897.
[2] H. Ammari, E. Bonnetier, E., Y. Capdeboscq, M. Tanter, and M. Fink, Electrical impedance tomography by elastic deformation, SIAM J. Appl. Math. 68 (2008), 1557–1573.
[3] H. Ammari, and H. Kang, Reconstruction of Small Inhomogeneities from Boundary Measurements, Lecture Notes in Math. 1846, Springer-Verlag, Berlin, 2004.
[4] H. Ammari, and H. Kang, Boundary layer techniques for solving the Helmholtz equation in the presence of small inhomogeneities, J. Math. Anal. Appl., 296 (2004), 190–208.
[5] H. Ammari, O. Kwon, J.K. Seo, and E. J. Woo, T-scan electrical impedance imaging system for anomaly detection, SIAM J. Appl. Math., 65 (2004), 252–266.
[6] D.C. Barber, and B.H. Brown, Applied potential tomography, J. Phys. Sci. Instrum., 17 (1984), 723–733.
[7] M. Cheney, and D. Isaacson, An overview of inversion algorithms for impedance imaging, Contemp. Math., 122 (1991), 29–39.
[8] M. Cheney, D. Isaacson, and J.C. Newell, Electrical impedance tomography, SIAM Rev., 41 (1999), 85–101.
[9] V.A. Cherepenin, A. Karpov, A. Korjenevsky, V. Kornienko, A. Mazaletskaya, D. Mazourov, and D. Meister, A 3D electrical impedance tomography (EIT) system for breast cancer detection, Physiol. Meas., 22 (2001), 9–18.
[10] E. Eyuboglu, R. Reddy, and J.S. Leigh, Imaging electrical current density using nuclear magnetic resonance, Elektrik, 6 (1998), 201–14.

[11] H. Gamba, D. Bayford, and D. Holder, Measurement of electrical current density distribution in a simple head phantom with magnetic resonance imaging, Phys. Med. Biol., 44 (1999), 281–91.

[12] M.L. Joy, V.P. Lebedev, and J.S. Gati, Imaging of current density and current pathways in rabbit brain during transcranial electrostimulation, IEEE Trans. Biomed. Eng., 46 (1999), 1139–1149.

[13] S. Kim, O. Kwon, J.K. Seo, and J.R. Yoon, On a nonlinear partial differential equation arising in magnetic resonance electrical impedance tomography, SIAM J. Math. Anal., 34 (2002), 511–526.

[14] Y.-J. Kim, O. Kwon, J.K. Seo, and E. J. Woo, Uniqueness and convergence of conductivity image reconstruction in magnetic resonance electrical impedance tomography, Inverse Problems, 19 (2003), 1213–1225.

[15] O. Kwon, J.K. Seo, and J.-R. Yoon, A real-time algorithm for the location search of discontinuous conductivities with one measurement, Comm. Pure Appl. Math., 55 (2002), 1–29.

[16] O. Kwon, E.J. Woo, J.-R. Yoon, and J.K. Seo, Magnetic resonance electrical impedance tomography (MREIT): Simulation study of J-substitution algorithm, IEEE Trans. Biomed. Eng., 49 (2002), 160–167.

[17] J.-Y. Lee, A reconstruction formula and uniqueness of conductivity in MREIT using two internal current distributions, Inverse Problems, 20 (2004), 847–858.

[18] N. Mandache, Exponential instability in an inverse problem for the Schrödinger equation, Inverse Problems, 17 (2001), 1435–1444.

[19] A.I. Nachman, Global uniqueness for a two-dimensional inverse boundary value problem, Ann. of Math, 143 (1996), 71–96.

[20] G.C. Scott, M.L. Joy, R.L. Armstrong, and R.M. Henkelman, Measurement of nonuniform current density by magnetic resonance, IEEE Trans. Med. Imaging, 10 (1991), 362–374.

[21] G.C. Scott, M.L. Joy, R.L. Armstrong, and R.M. Henkelman, Sensitivity of magnetic-resonance current density imaging, J. Magn. Reson., 97 (1992), 235–254.

[22] J. Sylvester, and G. Uhlmann, A global uniqueness theorem for an inverse boundary value problem. Ann. of Math. (2) 125 (1987), no. 1, 153–169.

[23] E.J. Woo, J.G. Webster, and W.J. Tompkins, A robust image reconstruction algorithm and its parallel implementation in electrical impedance tomography, IEEE Trans. Med. Imaging, 12 (1993), 137–146.

[24] T. Yorkey, J. Webster, and W. Tompkins, Comparing reconstruction algorithms for electrical impedance tomography, IEEE Trans. Biomed. Eng., 34 (1987), 843–852.